

# FATIGUE CRACK GROWTH BEHAVIOR OF MICRO-SIZED SPECIMENS PREPARED FROM AMORPHOUS ALLOY THIN FILMS

K. Takashima<sup>1</sup>, Y. Higo<sup>1</sup> and M. V. Swain<sup>2</sup>

<sup>1</sup> Precision and Intelligence Laboratory, Tokyo Institute of Technology,  
4259 Nagatsuta, Midori-ku, Yokohama 226-8503, Japan.

<sup>2</sup> Faculty of Dentistry and Department of Mechanical & Mechatronic Engineering,  
The University of Sydney, Australian Technology Park, Everleigh NSW 1430, Australia.

## ABSTRACT

Fatigue crack growth tests have been performed on micro-sized Ni-P amorphous alloy specimens to investigate the size effects on fatigue crack growth behavior of such micro-sized specimens. Two types of cantilever beam type micro-sized specimens with different breadth ( $10 (B) \times 12 (W) \times 50 (L) \mu\text{m}^3$  and  $30 (B) \times 12 (W) \times 50 (L) \mu\text{m}^3$ ) were prepared from an electroless plated Ni-P amorphous alloy thin film by focused ion beam machining. Notches with a depth of  $3 \mu\text{m}$  were introduced in the specimens. Fatigue crack growth tests were performed using a newly developed fatigue testing machine for micro-sized specimens in air at room temperature under constant load amplitude and stress ratios of 0.1, 0.3, 0.5 and 0.7. Striations were observed on the fatigue fracture surfaces and fatigue crack propagation rates were estimated by careful measurements of the striation spacings. The fatigue crack growth rates at stress ratios of 0.3 and 0.5 were higher than that at 0.1. This suggests that crack closure may occur even in such micro-sized specimens. The fatigue crack growth resistance is also dependent on the specimen breadth. This suggests that the stress state ahead of the crack may affect the crack growth behavior. The results obtained in this investigation provide basic guidelines for designing actual MEMS devices.

## KEYWORDS

Micro-sized specimen, Fatigue, Crack growth, Amorphous alloy, Thin film, Size effect

## INTRODUCTION

Many micro-sized components are involved in microelectromechanical systems (MEMS) and these components are subjected to cyclic loading as they move. These micro-sized components are usually fabricated from a thin film deposited on a substrate using suitable surface micromachining techniques. The evaluation of fatigue properties for thin films is thus extremely important to design reliable and long-term durable MEMS devices. For example, the components used in micro-optical mirrors and switches are considered to experience extremely high number of cyclic loads (over  $10^8$  cycles). To date, fatigue tests for thin films and fatigue life of such films have been investigated [1-3]. However, there

have been no data for fatigue crack growth properties which are important for actual MEMS devices. This is partly due to the lack of suitable fatigue testing machine for micro-sized materials. In our previous investigations, we have designed a new fatigue testing machine for micro-sized specimens [4, 5], and fatigue life curves have been obtained for micro-sized specimens prepared from a Ni-P amorphous alloy thin film [6].

Amorphous alloy thin films deposited on substrates by sputtering or plating techniques are considered to be potential candidate materials for MEMS devices because of their isotropic mechanical properties and high corrosion resistance. Therefore, it is important to clarify the fatigue crack growth properties of these amorphous thin films. However, the fatigue properties of micro-sized amorphous specimens have not yet been studied apart from our previous investigation on the fatigue life of a micro-sized Ni-P amorphous alloy specimens [6]. In this investigation, fatigue crack growth tests have been performed on micro-sized specimens prepared from an electroless deposited Ni-P amorphous alloy thin film and the size effects on the fatigue crack growth behavior of micro-sized specimens have been discussed.

## EXPERIMENTAL PROCEDURE

### *Preparation of Specimens*

The material used in this investigation was a Ni-11.5 mass%P amorphous thin film electroless plated on an Al-4.5 mass%Mg alloy. The thickness of the amorphous layer was 12  $\mu\text{m}$  and that of the Al-4.5 mass%Mg alloy substrate was 0.79 mm, respectively. A disk with a diameter of 3 mm was cut from the Ni-P/Al-Mg sheet by electro discharge machining. An amorphous layer was separated from the Al-Mg alloy substrate by dissolving the substrate with a NaOH aqueous solution. The amorphous thin film was fixed on a holder and two types of micro-cantilever beam specimens with dimensions of 10 ( $B$ )  $\times$  12 ( $W$ )  $\times$  50 ( $L$ )  $\mu\text{m}^3$  and 30 ( $B$ )  $\times$  12 ( $W$ )  $\times$  50 ( $L$ )  $\mu\text{m}^3$  were cut from the amorphous layer by focused ion beam machining. Figures 1 (a) and (b) show the specimens prepared by the above procedures. Notches with a depth of 3  $\mu\text{m}$  were introduced into the specimens by focused ion beam machining. This notch depth is equivalent to  $a/W = 0.25$ , where  $a$  is notch length and  $W$  is specimen width. The width of the notch was 0.5  $\mu\text{m}$ , and the notch radius is thus deduced to be 0.25  $\mu\text{m}$ . The notch position was 10  $\mu\text{m}$  away from the fixed end of the specimen. The loading position is set at 40  $\mu\text{m}$  from the fixed end of the specimen.

### *Fatigue Crack Growth Test*

Fatigue crack growth tests were performed in air at room temperature using the fatigue testing machine for micro-sized specimens. Fatigue tests were carried out at a frequency of 10 Hz and different stress ratios,  $R$  ( $R = P_{\min} / P_{\max}$ , where  $P_{\min}$  is the minimum load and  $P_{\max}$  is the maximum load applied over the fatigue cycle) of 0.1, 0.3, 0.5 and 0.7 under constant load amplitude ( $\Delta P/2$ , where  $\Delta P = P_{\max} - P_{\min}$ ) of 2 mN. This fatigue test condition was determined from our preliminary experiments. Although the crack length was not able to be measured directly in this testing machine, the change in specimen compliance

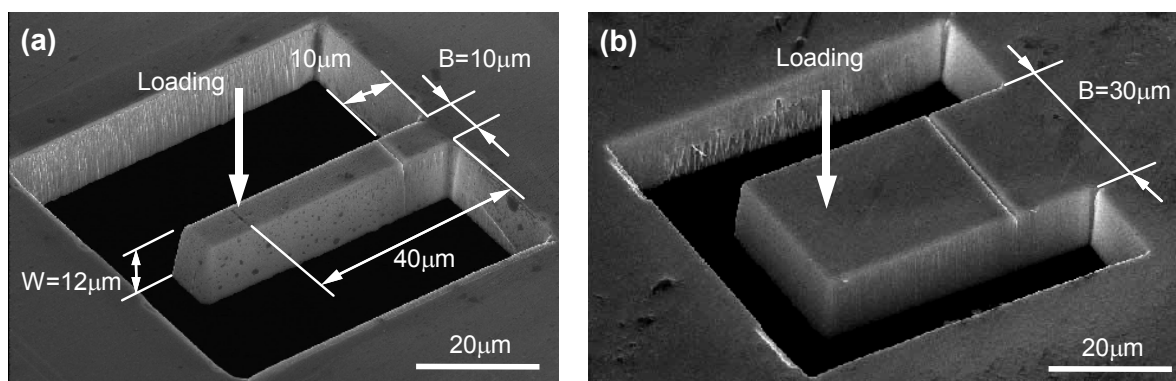


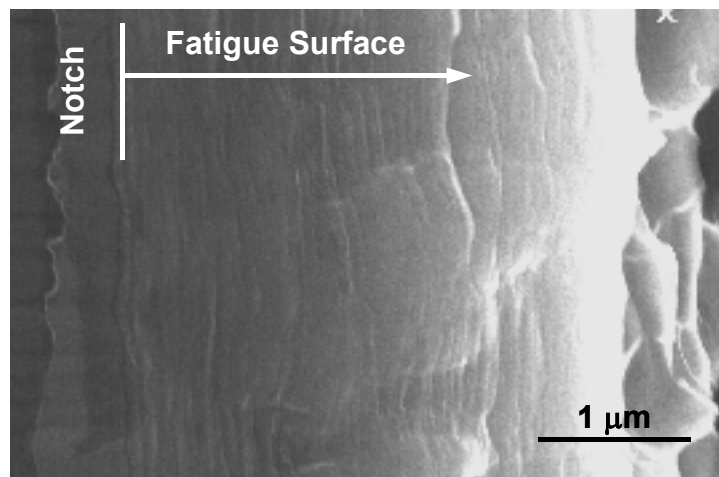
**Figure 1:** Two types of micro-sized cantilever beam specimens with different breadth ( $B$ ) prepared by focused ion beam machining. (a)  $B=10\text{mm}$  and (b)  $B=30\text{mm}$ .

can be measured during fatigue tests. The initiation of crack growth was then determined by monitoring the specimen compliance. The fatigue surfaces after the tests were observed using a HITACHI S-4000 field emission-gun type scanning electron microscope.

## RESULTS AND DISCUSSION

### *Fatigue Crack Growth Behavior*

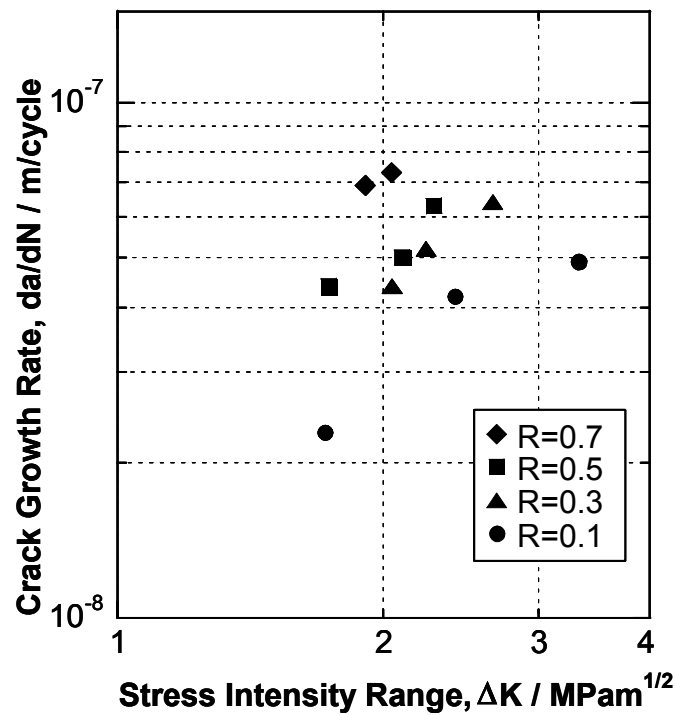
Figure 2 shows a scanning electron micrograph of fracture surface for the specimens with a breadth,  $B$ , of  $10\ \mu\text{m}$  after a fatigue crack growth test at a stress ratio of 0.5. The fracture surface is relatively flat and very fine equispaced markings are clearly visible ahead of the notch. These markings have been considered to be striations [7]. If the spacing between the striations on the fatigue surface is assumed to be equivalent to the fatigue crack growth rate, a fatigue crack growth resistance curves can be obtained from the measurements of the striation spacings. Careful measurements of the striation spacings were then made and fatigue crack growth rates ( $da/dN$ ) as a function of applied stress intensity factor range ( $\Delta K$ ) (where  $\Delta K = K_{\text{max}} - K_{\text{min}}$ ) were obtained. Stress intensity factor ( $K$ ) is calculated from the equation for a single edge notched cantilever beam specimen [8]. The crack length,  $a$ , was measured from scanning electron micrographs of the fatigue surfaces.



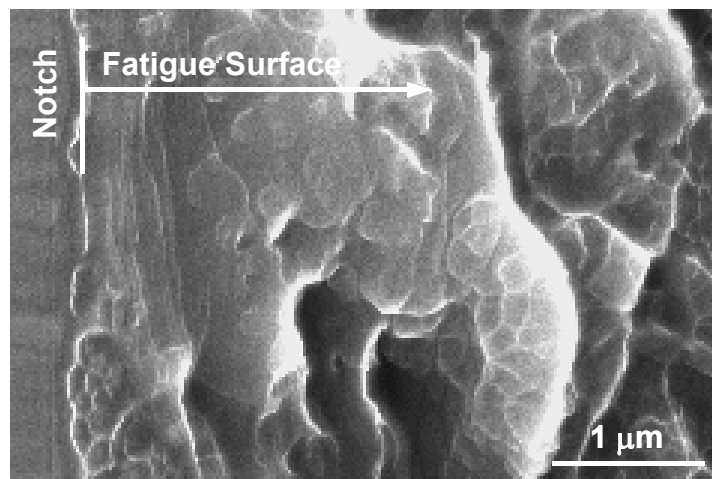
**Figure 2:** Scanning electron micrograph of fatigue surface. Fine equispaced markings considered to be striations are observed. Crack growth direction is from left to right.

Figure 3 shows the fatigue crack growth resistance curves for the specimens with  $B$  of  $10\ \mu\text{m}$  at different stress ratios. The fatigue crack growth rates at a stress ratio of 0.3 and 0.5 are almost the same. In contrast, the fatigue crack growth rate at a stress ratio of 0.1 is lower than those at 0.3 and 0.5 at a given value of  $\Delta K$ . Generally, a decrease in fatigue crack growth rate at a low stress ratio can be explained by crack closure effects for ordinary sized specimens. This suggests that crack closure effects may occur even in such micro-sized specimens and may affect the fatigue crack growth behavior. The fatigue surface is relatively flat as shown in Fig. 2, so this crack closure is deduced to be a plasticity-induced crack closure.

On the other hand, the fatigue crack growth rate at a stress ratio of 0.7 is higher than those of 0.3 and 0.5. Figure 4 shows a fatigue surface at a stress ratio of 0.7. The fatigue surface is very rough and some vein patterned regions are observed in addition to the striation pattern. At this stress ratio,  $K_{\text{max}}$  was  $6.8\ \text{MPam}^{1/2}$  and this value is close to  $K_Q$  value of the specimen [9]. Therefore, the crack is deduced to extend by both cyclic and static mode, and this resulted in higher crack growth rate at a stress ratio of 0.7.



**Figure 3:** Fatigue crack growth resistance curves for micro-sized specimens at different stress ratios.



**Figure 4:** Scanning electron micrograph of fatigue surface tested at a stress ratio of 0.7. Crack growth direction is from left to right.

#### ***Effect of Specimen Breadth on Fatigue Crack Growth***

In order to investigate the effect of stress state ahead of the crack tip on the fatigue crack growth behavior of micro-sized specimens, fatigue crack growth tests for specimens with different breadth ( $B$ ) were carried out. Figure 5 shows a fatigue crack growth resistance curves at a stress ratio of 0.5, at which no closure effect is assumed, for the specimens with  $B$  of 10 and 30  $\mu\text{m}$ , respectively. The fatigue crack growth rate with  $B$  of 10  $\mu\text{m}$  is higher than that with  $B$  of 30  $\mu\text{m}$ . In our previous investigations [9], plane stress and plane strain regions were observed on fracture surfaces even in micro-sized specimens. Thus, a decrease in crack growth rate with an increase in specimen breadth may be due to the difference in stress state ahead of the crack. It is interesting that the effect of specimen breadth on fatigue crack growth behavior was observed even in such micro-sized specimens.

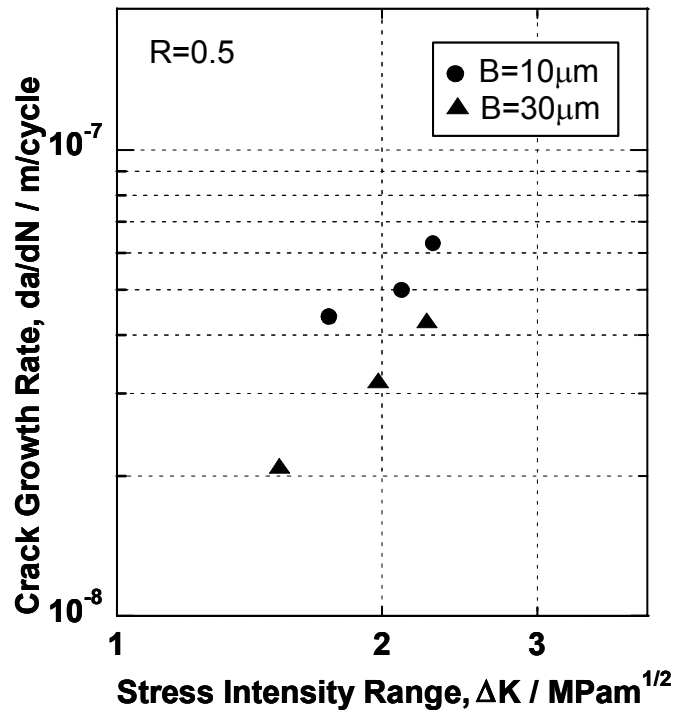


**Figure 5:** Fatigue crack growth resistance curves for the specimens with different  $B$  tested at a stress ratio of 0.5.

### *Effect of Specimens Size on Fatigue Crack Growth*

As shown in Fig. 3, the effect of stress ratio on fatigue crack growth, which is deduced to be associated with a crack closure effect, is observed even for micro-sized specimens. The length of crack extended by fatigue loading in the micro-sized specimens used in this investigation was only 2 - 3  $\mu\text{m}$  as shown in Fig. 2. Generally, crack closure effects are less pronounced for short cracks with length of less than 100  $\mu\text{m}$  and almost no closure effects are observed for extremely short cracks with length in the order of microns [10]. However, these observations have been obtained for short cracks in ordinary-sized specimens. In contrast, the size of the specimen used in this investigation is three dimensionally small, so the normalized crack length is sufficiently long compared to the specimen size (actually,  $a/W$  is approximately over 0.5 at final fracture). Therefore, the crack length of 2 - 3  $\mu\text{m}$  should be regarded as a long crack for this size of specimen, so the closure effects are deduced to be pronounced even for micro-sized specimens.

In this investigation, the fatigue crack growth behavior for micro-sized specimen was clarified. However, the detail of size effects on fatigue crack growth behavior is still unclear. Further investigation is required to quantify the size effect on fatigue mechanisms in micro-sized specimens.

## CONCLUSIONS

Fatigue crack growth tests have been performed for micro-sized cantilever beam type specimens prepared from an electroless plated Ni-P amorphous alloy thin film to investigate the size effects on fatigue crack growth behavior of such micro-sized specimens.

Striations were observed on the fatigue fracture surfaces and fatigue crack propagation rates were estimated by a careful measurement of the striation spacing. The fatigue crack growth rates at stress ratios of 0.3 and 0.5 were almost identical, but the fatigue crack growth rate at stress ratio of 0.1 were lower compared to that at 0.3 and 0.5 at a given value of  $\Delta K$ . This suggests that crack closure may occur even in such micro-sized specimens. In contrast, the fatigue crack growth rate at a stress ratio of 0.7 was

higher than those at 0.3 and 0.5. The fatigue crack was extended by both cyclic and static loading and this causes higher fatigue crack growth rate at a stress ratio of 0.7. The results obtained in this investigation are the first measurements of fatigue crack growth properties for micro-sized specimens and provide basic guidelines for design of actual micro-sized machine and MEMS devices.

### ***Acknowledgement***

This work was partly supported by the Grant-in-Aid for Scientific Research (B) (2) No. 12555186 from the Ministry of Education, Science, Sports and Culture, Japan. The authors would like to thank to Mr. S. Maekawa for his help in experiments.

### **REFERENCES**

1. Read, D. T. and Dally, W. (1995) *J. Electronic Packaging*, **117**, 1.
2. Muhlstein, C. L. and Brown, S. (1998). In: *Tribology Issues and Opportunities in MEMS*, pp. 529-538, Bhusan, B., Kluwer Academic Publications, Dordrecht.
3. Schwaiger, R. and Kraft, O. (1999) *Scripta Mater.*, **41**, 823.
4. Takashima, K., Kimura, T., Shimojo, M., Higo, Y., Sugiura, S. and Swain, M. V. (1999). In: *Fatigue '99 (Proc. 7th Int. Fatigue Cong.)*, pp. 1871-1876, Wu, X-R. and Wang, Z-G., (Eds). Higher Education Press, Beijing.
5. Higo, Y., Takashima, K., Shimojo, M., Sugiura, S., Pfister, B. and Swain, M. V. (2000). In: *Materials Science of Microelectromechanical Systems (MEMS) Devices II*, pp. 241-246, deBoer, M. P., Heuer, A. H., Jacobs, S. J. and Peeters, E., (Eds). The Materials Research Society, Pennsylvania.
6. Maekawa, S., Takashima, K., Shimojo, M., Higo, Y., Sugiura, S., Pfister, B. and Swain, M. V. (1999) *Jpn. J. Appl. Phys.*, **38**, 7194.
7. Maekawa, S., Takashima, K., Shimojo, M., Higo, Y. and Swain, M. V. (2000). In: *Materials Science of Microelectromechanical Systems (MEMS) Devices II*, pp. 247-252, deBoer, M. P., Heuer, A. H., Jacobs, S. J. and Peeters, E., (Eds). The Materials Research Society, Pennsylvania.
8. Okamura, H. (1976). *Introduction to Linear Fracture Mechanics*, Baifukan, Tokyo, (in Japanese).
9. Ichikawa, Y., Maekawa, S., Takashima, K., Shimojo, M., Higo, Y. and Swain, M. V. (2000). In: *Materials Science of Microelectromechanical Systems (MEMS) Devices II*, pp. 273-278, deBoer, M. P., Heuer, A. H., Jacobs, S. J. and Peeters, E., (Eds). The Materials Research Society, Pennsylvania.
10. Suresh, S. (1991), *Fatigue of Materials*, Cambridge University Press, Cambridge.